

Observation-based Optimal Control Law Learning with LQR Reconstruction

Chendi Qu, Jianping He, Xiaoming Duan

Abstract—Designing controllers to generate various trajectories has been studied for years, while recently, recovering an optimal controller from trajectories receives increasing attention. In this paper, we reveal that the inherent linear quadratic regulator (LQR) problem of a moving agent can be reconstructed based on its trajectory observations only, which enables one to learn the optimal control law of the agent autonomously. Specifically, the reconstruction of the optimization problem requires estimation of three unknown parameters including the target state, weighting matrices in the objective function and the control horizon. Our algorithm considers two types of objective function settings and identifies the weighting matrices with proposed novel inverse optimal control methods, providing the well-posedness and identifiability proof. We obtain the optimal estimate of the control horizon using binary search and finally reconstruct the LQR problem with above estimates. The strength of learning control law with optimization problem recovery lies in less computation consumption and strong generalization ability. We apply our algorithm to the future control input prediction and the discrepancy loss is further derived. Numerical simulations and hardware experiments on a self-designed robot platform illustrate the effectiveness of our work.

I. INTRODUCTION

Nowadays, as the development of localization, computer vision and planning, mobile agents have been widely applied in various fields and achieved high-profile success [2]. Lots of studies focus on designing controllers to generate satisfying trajectories [3], while in this paper we pay attention to its inverse problem: *How to learn the interior controller based on agent's trajectory observations?*

To tackle this problem, let's consider a mobile agent driving from its initial position to a target point, which is one of the most common and basic scenarios of agents. In most situations, the agent is exposed to the physical world thus its trajectory can be observed by potential external attackers [4]–[6]. We suppose there is another agent equipped with camera and computation ability trying to learn the trajectory and motion of the agent based on observations only. The issue that agents learn from other agents through observations is similar to learning from demonstration (LfD) [7], [8], while in our case the agent needs to collect data actively instead of just being provided by human demonstrations. LfD has raised extensive studies recent years and applied to various fields including autonomous driving [9], manufacturing [10] and human-robot interaction [11]. Given standard demonstrations,

one mainstream category of LfD algorithms is to learn the control policy directly from the state observations to action [12], [13], known as end-to-end learning. However, this branch of methods usually require for large amount of demonstrations as training data and contain little generalization ability between different environments.

Therefore, our approach is to conduct a two-stage LfD, learning the interior controller of the agent first, which is a non-trivial problem, since the control objective of the agent is unknown. To further simplify the problem, we assume the moving agent is utilizing an LQR controller [14]. Since LQR is a state-feedback controller, the control law is actually a series of feedback gain matrices. Note that if the controller is infinite-time, these matrices are invariant and can be estimate with the optimal state and input trajectories. However, in the finite-time case, this sequence of matrices is time invariant with unknown length. Thus, in our paper the main idea is to reconstruct the control optimization problem. Once the optimization problem is recovered, we can obtain the control law and imitate the agent's motion with strong generalization performance. Assuming the dynamic model and objective function form is known, to reconstruct the LQR problem, we need to obtain the target state, the weighting matrices and the control horizon.

An inspiring two-stage LfD method is inverse optimal control (IOC) [15], [16], which is utilized to identify objective function parameters being an important part of our algorithm. IOC algorithms diverse according to the assumption of the objective function form. As for the quadratic LQR form considered in our case, [17], [18] both study the infinite-time problem assuming the constant control gain matrix is already known, while we provide the gain matrix estimator. In addition, [19], [20] propose approaches to identify objective function as continuous finite-time LQR and [21], [22] solve IOC problems for discrete-time. However, few of these studies consider the classic LQR setting including final-state, process-state and process-cost terms with different parameters, and they usually require complete trajectory observations. The past research on control horizon has mainly focused on adaptive horizon model prediction control. The control stability and effectiveness of the system can be decided by the horizon length [23] and the horizon estimation refers to choosing an optimal length to balance the performance and computation cost [24], [25]. However in our paper, we study how to identify the horizon length of the optimization problem given optimal state trajectory observations with noises.

One important application of our optimization problem

The authors are with the Dept. of Automation, Shanghai Jiao Tong University, and Key Laboratory of System Control and Information Processing, Ministry of Education of China, Shanghai, China. E-mail address: {qucd21, jphe, xduan}@sjtu.edu.cn.

Part of this paper has been accepted to IFAC 2023 World Congress [1].

reconstruction algorithm is the control input and trajectory prediction, which can be the basis for attacker’s subsequent attacks, interception or misleading. Some existing methods for trajectory prediction are data-driven and model-free, such as using polynomial regression [26], [27] or introducing neural networks, including the long short-term memory neural network [28] or graph neural network [29]. However, these usually require a large amount of observations as well as the model training in the early stage. Another class of algorithms is model-based. For instance, [30] use an unscented Kalman filter to predict multi-agent trajectories. [31] measure the secrecy of the trajectory and proves that uniform distributed inputs maximize the unpredictability of the system. But these predictive models often assume that the control inputs at each step are known, which in our case, cannot be obtained directly. Notice that if we build the reconstructed optimization problem of the agent, we are able to calculate the input at arbitrary states and predict the future trajectory accurately, combining with the estimation of the dynamic model and current state through system identification (SI) [32] and data fusion filters [33], [34], respectively.

Motivated by above discussion, we design a control law learning algorithm with LQR problem reconstruction based on trajectory observations. We first estimate the target point by finding the intersection of the trajectory extension lines. Then identify the weighting matrices in the objective function with IOC algorithms and obtain the optimal horizon estimate through a binary search method. Finally, we reconstruct the control optimization problem and solve its solution as the learned control law. This algorithm can not only learn the control law and enable agents to imitate the motion from arbitrary initial states, but to predict the future input and state trajectory of the mobile agent precisely. One of the main challenges of problem reconstruction is how to build a proper IOC problem to identify the parameters simultaneously in complex quadratic objective function forms. Another lies in analyzing the estimation error of each part and their impact on the input prediction application.

This paper is an extension of our conference paper [1]. The main differences include i) we reorganize the article structure to focus on LQR problem reconstruction, treating input prediction as an application, ii) the infinite-time case is considered, iii) the IOC problem for more complex form of the objective function is built and solved, iv) the sensitivity analysis of control horizon estimation is provided, v) extended simulations are provided and hardware experiments are added. The main contributions are summarized as follows:

- We investigate the observation-based optimal control law learning issue and propose a novel LQR reconstruction algorithm for mobile agents, including the estimation of target state, objective function parameters and the control horizon. As far as we know, we are the first to consider and reveal that the entire optimization LQR problem can be recovered based on only observations.
- We solve the IOC problem considering two forms of objective functions, including i) final-state only setting

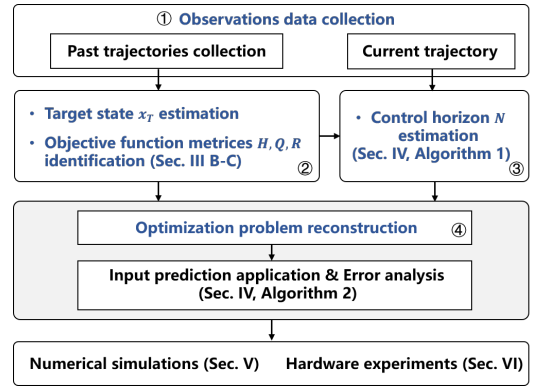


Fig. 1. Road-map of this paper.

based on PMP conditions given incomplete state trajectories and ii) classic LQR setting based on condition number minimization. We provide the scalar ambiguity property analysis and further prove the uniqueness and identifiability of the problem. Furthermore, a novel approach for estimating the agent’s control horizon is presented, converting a non-convex integer optimization into a binary search problem.

- We apply our LQR reconstruction algorithm to the future control inputs prediction problem, providing error sensitivity analysis based on the convergent property of the algebraic Riccati equation.
- Numerical simulations reveals the effectiveness of both objective parameters and control horizon estimations. Our algorithm shows low bias and variance of the error. Moreover, hardware experiments of input prediction conducted on our self-designed robot platform demonstrate the prediction accuracy and efficiency.

The remainder of the paper is organized as follows. Section II describes the problem of interest. Section III analyzes the infinite-time case and studies the objective function identification in two settings. Section IV estimates the control horizon and summarizes the complete algorithm flow. Simulation results and hardware experiments are shown in Section V-VI, followed by the conclusion in Section VII.

II. PRELIMINARIES AND PROBLEM FORMULATION

A. Model Description

Consider a mobile agent R_m driving from its initial state to a fixed target point x_T . R_m is modeled by a discrete-time linear system

$$x_{k+1} = Ax_k + Bu_k, \quad (1)$$

where x_k is the state vector, u_k is the control input and A, B are $n \times n$ and $n \times m$ matrices. Assume that (A, B) is controllable and B has full column rank. Moreover, A is an invertible matrix since the system matrix of a discrete-time system sampled from a continuous linear system is always invertible [22]. The output function is

$$y_k = Cx_k + \omega_k, \quad (2)$$

TABLE I
NOTATION DEFINITIONS

Symbol	Definition
$\hat{x}_{k k}$	the estimation of state x_k at time k ;
$\hat{u}_{k k}$	the prediction of input u_k at time k ;
x_T	the set target state;
$A^c(A_k^c)$	the closed-loop system matrix (at time k);
$K(K_k)$	the feedback gain matrix of LQR problem (at time k);
$K_{i:j}$	a matrix sequence $\{K_i, K_{i+1}, \dots, K_j\}$;
N	the control horizon of a control process;
M	the number of trajectories in the observation data;
$l(l_j)$	the length of a single (j -th) observation trajectory;
\mathcal{Y}^j	the j -th observation trajectory;
\mathcal{X}^j	the state sequence estimated from observation \mathcal{Y}^j ;
$A(i, j)$	The i -th row and j -th column element in matrix A ;
$A(:, j)$	The j -th column of matrix A ;
A^\dagger	Pseudo-inverse of matrix A ;
I_n	an $n \times n$ dimensional identity matrix;
$\ \cdot\ $	the 2-norm of a vector;

where y_k is the outputs such as agent's position and $C \in \mathbb{R}^{p \times n}$ is the observation capability matrix. We require C is invertible in our algorithm and analysis since if C is a fat matrix ($p < n$), the information contained in x_t cannot be fully characterized by y_t and the identification will be difficult [35]. $\omega_k \sim \mathcal{N}(0, \Gamma)$ is independent Gaussian observation noise. There is

$$\mathbb{E}(\omega_k) = 0, \mathbb{E}(\|\omega_k\|^2) < +\infty. \quad (3)$$

Note that R_m follows the optimal LQR control and the optimization problem is described as

$$\begin{aligned} \mathbf{P}_0 : \min_{u_{0:N-1}} J_0 &= \frac{1}{2} x_N^T H x_N + \sum_{k=0}^{N-1} \frac{1}{2} (x_k^T Q x_k + u_k^T R u_k), \\ \text{s.t. } (1), x_0 &= \bar{x} - x_T, \end{aligned}$$

where H, R are positive definite matrices, Q is a semi-positive definite matrix and \bar{x} is the initial state. The first term in objective function J_0 reflects the deviation to the target state and the second term represents the cost of energy during the process. To simplify the problem description, we assume the agent sets the target as 0 in \mathbf{P}_0 and performs coordinate system transformation on the initial state \bar{x} with x_T . It is known that the solution of \mathbf{P}_0 is

$$u_k = -K_k x_k, k = 0, 1, \dots, N-1, \quad (5)$$

where $K_{0:N-1} = \{K_0, K_1, \dots, K_{N-1}\}$ is the control gain matrix sequence related to the system equation and control objectives, which is calculated through the iterative equations (13) shown in Section III-C.

B. Problem Formulation

Now there is another external agent R_o observing and recording the output trajectories of R_m . We assume R_o has exact knowledge of the dynamic function, which can be accessed by SI methods, and the quadratic form of the objective

function. Suppose that R_o obtains $M \geq n$ optimal trajectories $\{\mathcal{Y}^1, \dots, \mathcal{Y}^M\}$ of R_m , where

$$\mathcal{Y}^j = \{y_0^j, y_1^j, \dots, y_{l_j}^j\}, j = 1, 2, \dots, M,$$

is the j -th trajectory and $l_j + 1 \geq 2n$ is the length.

Assumption 1. We require there exist at least n linearly independent final states among M trajectories, which means the matrix $[y_{l_1}^1 \dots y_{l_M}^M]$ has a full row rank.

Consider that R_o tries to learn the control law of R_m based on observations, which is equal to estimate the control feedback gain matrix sequence $K_{0:N-1}$ of \mathbf{P}_0 accurately. However, this is a non-trivial problem since K_k is time-variant and the control objective of R_m is unknown. Therefore, the main idea of this paper is to reconstruct the optimization problem \mathbf{P}_0 in order to solve $K_{0:N-1}$ directly, which means we need to estimate the following unknown parameters:

- target state x_T ;
- weighting matrices in objective function H, Q, R ;
- control horizon length N .

If the above estimations are accurate, we can obtain the real control law of R_m accurately by solving the reconstructed optimization problem. Notice that the target state estimation is quite trivial and less important in our problem reconstruction. We have the following remark.

Remark 1. To estimate the target state, we can do curve fitting on at least two non-parallel observed trajectories, whose intersection is calculated as the estimate \hat{x}_T . Moreover, one simple way is to directly observe the final state in multiple trajectories and take the average as the target value.

Hence, in the following sections, we will estimate the objective function parameters and control horizon accordingly, and then formulate the optimization problem with all the estimates.

III. OBJECTIVE FUNCTION IDENTIFICATION

In this section, we will firstly discuss the control law learning in the infinite horizon case as an inspiration. Then, we focus on finite-time problem and estimate the weighting parameters in the objective function through IOC methods. Since in some situations, the agent only pays attention to whether the target state can be reached and the whole energy consumption during the process instead of the transient states. Therefore, we will first consider the final-state only setting based on looser data assumptions. In the third subsection, we will solve the classic LQR setting IOC problem.

A. Infinite Horizon Case

When the control horizon N of agent R_m goes to infinity, the objective function in \mathbf{P}_0 changes into

$$J^\infty = \frac{1}{2} \sum_{k=0}^{\infty} (x_k^T Q x_k + u_k^T R u_k).$$

and the optimal control law K is given by

$$K = (R + B^T P B)^{-1} B^T P A, \quad (6)$$

where the intermediate parameter P satisfies the following Riccati equation:

$$P = A^T P A - A^T P B (R + B^T P B)^{-1} B^T P A + Q.$$

Since in the infinite case, the feedback gain matrix K is constant, we can estimate K based on observations directly without the control problem reconstruction.

Denote the closed-loop system matrix $A^c = A - BK$ and its spectral radius satisfies $\rho(A^c) < 1$. We have

$$y_{k+1} = C A^c C^{-1} (y_k - \omega_k) + \omega_{k+1}$$

for all k , which is a typical form of first-order stationary vector auto-regression process. We can calculate A^c inspired by ordinary least square (OLS) method with one single trajectory \mathcal{Y}^1 . The estimator is designed as

$$\hat{A}^c = C^{-1} \left(\frac{1}{l} Y X^T \right) \left(\frac{1}{l} X X^T - I_l \otimes \Gamma \right)^{-1} C, \quad (7)$$

where $X = (y_0^1, y_1^1, \dots, y_{l-1}^1)^T$, $Y = (y_1^1, y_2^1, \dots, y_l^1)^T$ and $\Gamma = \text{diag}\{\sigma_{\omega,1}^2, \dots, \sigma_{\omega,p}^2\}$. The matrix $X^T X$ is required to be full rank to guarantee the uniqueness.

Then, we learn the constant gain matrix

$$\hat{K} = B^\dagger (A - \hat{A}^c). \quad (8)$$

as control law. The error between the estimation and the true K can be restricted by:

$$\begin{aligned} \|K - \hat{K}\|_F &= \|B^\dagger (A - A^c) - B^\dagger (A - \hat{A}^c)\|_F \\ &\leq \|B^\dagger\|_F \|\hat{A}^c - A^c\|_F \leq \|B^\dagger\|_F \cdot \sqrt{n} \|\hat{A}^c - A^c\|. \end{aligned}$$

According to Theorem 6 in [36], the estimation error of gain matrix K converges to zero as the number of samples l goes larger, which is

$$\lim_{l \rightarrow \infty} \|\hat{A}^c - A^c\| = 0, \quad \|\hat{A}^c - A^c\| \sim \mathcal{O}\left(\frac{1}{\sqrt{l}}\right). \quad (9)$$

The control law learning in infinite case is quite trivial but inspiring, revealing that the feedback gain matrix K can be obtained through OLS-like estimators. In the next subsections, we will turn back to the finite-time problem.

B. Final-state Only Setting

In this subsection, We study a simplified objective function setting without considering the penalties on states $x_k^T Q x_k$ (i.e., $Q = 0$) described as

$$J_1 = \frac{1}{2} (x_N^T x_N + \sum_{k=0}^{N-1} u_k^T R u_k). \quad (10)$$

We set $H = I$ in the sense that for minimizing the distance between the final state and the target point, the weights on each component of x_N are usually considered equal. Then, the IOC problem here is to estimate the parameters R only with M optimal state trajectories in the presence of observation noises. We have nothing requirements for data other than Assumption 1, which means these M trajectories can be just fragments of some complete state trajectories.

According to the Pontryagin's minimum principle (PMP) [37], we introduce the following lemma:

Lemma 1. Consider the optimization problem \mathbf{P}_0 with J_1 . The optimal control inputs $u_{0:N-1}^*$ and its corresponding state trajectories $x_{0:N}^*$ satisfy

- 1) optimal control policy $u_i^* = -R^{-1} B^T \lambda_{i+1}^*$,
- 2) costate equation $\lambda_i^* = A^T \lambda_{i+1}^*$,
- 3) terminal condition $\lambda_N^* = H x_N^*$,

with the given initial state x_0^* , where λ_i is the costate of the system, $i = 0, 1, \dots, N-1$.

It is straightforward to find that \mathbf{P}_0 has the same optimal solution with objective functions J_1 and αJ_1 , $\alpha \in \mathbb{R}_+$. We provide following lemma to reveal that PMP conditions in Lemma 1 have this scalar ambiguity property as well.

Lemma 2. Suppose parameters $H, R, x_{1:N}^j, \lambda_{1:N}^j$ satisfy the PMP conditions, then $H' = \alpha H, R' = \alpha R, x_{1:N}^j, \alpha \lambda_{1:N}^j$ for $\alpha \in \mathbb{R}_+$ are also a set of solution to these conditions.

Proof. The proof is given in Appendix A. \square

Note that the PMP condition is the necessary condition for the optimal solution of \mathbf{P}_0 . We set PMP condition as the constraint and formulate the inverse control problem Problem 1 based on M trajectory observations $\{\mathcal{Y}^1, \dots, \mathcal{Y}^M\}$. Since there exist observation noises, $x_{1:N_j}$ and $\lambda_{1:N_j}$ are also optimization variables. Moreover, in our case we constrain $H = I$, then according to Lemma 2, the optimal solution to Problem 1 is supposed to be unique.

Problem 1. (Inverse Control Problem with PMP)

$$\begin{aligned} \min_{\hat{R}, x_{1:N_j}^j, \lambda_{1:N_j}^j} & \frac{1}{M} \sum_{j=1}^M \sum_{i=1}^{N_j} \|y_i^j - C x_i^j\|^2 \\ \text{s.t.} & \quad x_{i+1}^j = A x_i^j - B \hat{R}^{-1} B^T \lambda_{i+1}^j, \\ & \quad \lambda_i^j = A^T \lambda_{i+1}^j, \lambda_{N_j}^j = x_{N_j}^j, x_0^j = y_0^j - \hat{x}_T, \\ & \quad i = 0, 1, \dots, N_j - 1, j = 1, \dots, M. \end{aligned}$$

We offer the following theorem to further prove the well-posedness property of the problem, which means the inverse problem of \mathbf{P}_0 with J_1 exists a unique solution. Denote $A_k^c = A - BK_k$ as the close-loop system matrix at time k .

Theorem 1. Suppose two closed-loop system matrix sequences $A_{0:N-1}^c, A'_{0:N-1}$ are optimal solutions to problem \mathbf{P}_0 with $J_1(R)$ and $J_1(R')$ respectively. If we have $A_k^c = A'_k$ for all k , there is $R = R'$.

Proof. The proof is given in Appendix B. \square

Furthermore, we present Theorem 2 as follow to reveal that the solution of Problem 1 is the true value of R when the amount of observations is large enough.

Theorem 2. Suppose $\hat{R}, x_{1:N}^*, \lambda_{1:N}^*$ are the optimal solution to Problem 1. We have

$$\Pr\left(\lim_{M \rightarrow \infty} \|\hat{R} - R\| = 0\right) = 1.$$

Proof. The proof is given in Appendix C. \square

With the above theorems, we are able to obtain the objective function parameter estimate \hat{R} by solving the Problem 1.

C. Classic LQR Setting

Now we consider adding the process-state term into minimization and the objective function is written as

$$J_0 = \frac{1}{2}x_N^T H x_N + \sum_{k=0}^{N-1} \frac{1}{2}(x_k^T Q x_k + u_k^T R u_k). \quad (12)$$

Solving the optimization problem \mathbf{P}_0 , we obtain a sequence of time-varying gain matrices $K_{0:N-1}$ calculated by

$$K_k = (R + B^T P_{k+1} B)^{-1} B^T P_{k+1} A, \quad (13)$$

and P_k satisfies the following iterative equation with the initial value $P_N = H$:

$$P_k = K_k^T R K_k + (A - B K_k)^T P_{k+1} (A - B K_k) + Q. \quad (14)$$

Inspired by the infinite-time case in Section III-A, we propose an algorithm consisted of two parts: i) Estimate the feedback gain matrices \hat{K}_k first based on the observation trajectories; ii) Calculate a proper $(\hat{H}, \hat{Q}, \hat{R})$ with matrices \hat{K}_k . We will describe the two parts separately.

Remark 2. Notice that the form of J_0 subsumes J_1 ($Q = 0, H = I$) in the previous subsection. However, we still divide them and provide two different algorithms since for identifying J_1 there is no requirements on observations, which can only be a segment of the trajectory, while in this subsection we need the observation to be a whole trajectory containing the final state. This will be shown in the following part.

• Feedback Gain Matrices Estimation

Suppose we obtain M trajectory observations $\{\mathcal{Y}^1, \dots, \mathcal{Y}^M\}$. As Remark 2 saying, in this subsection we require the observation to contain the final state of each trajectory, which is not difficult to achieve since we have estimate the target state or we can just observe for enough long time waiting for the agent to get to its target. Then we take $l \leq \min\{l_1, \dots, l_M\}$ steps from the end of each trajectory and reorder them as

$$\bar{\mathcal{Y}}^j = \bar{y}_{0:l}^j = y_{l_j-1:l_j}^j.$$

Now we have a truncated trajectory set $\{\bar{\mathcal{Y}}^1, \dots, \bar{\mathcal{Y}}^M\}$ for subsequent estimation. Denote the closed-loop system matrix at time k as $A_k^c = A - B K_k$, then we have

$$y_{k+1} = C A_k^c x_k + \omega_{k+1} \quad (15)$$

for all k . Based on equations (13) and (14), we provide the following lemma:

Lemma 3. If H, Q, R remain unchanged, considering two complete optimal state trajectories $\{x_{0:N_1}^1\}, \{x_{0:N_2}^2\}$ with different control horizons $N_1 \leq N_2$ generated by the given system, we have matrix sequence $\{K_{N_1}^1, K_{N_1-1}^1, \dots, K_0^1\}$ equal to $\{K_{N_2}^2, K_{N_2-1}^2, \dots, K_{N_2-N_1}^2\}$.

Denote \mathcal{X}^j as the state sequence estimated from truncated trajectory $\bar{\mathcal{Y}}^j$. We utilize following method to estimate states \hat{x}_k from the observation y_k through a filter [21]. Denote $D = CB$. For $\{y_{0:l}\}$, there is

$$\begin{aligned} \zeta_{k+1} &= (A - ABD^\dagger C)\zeta_k + ABD^\dagger(y_k - CA^k x_0), \\ \hat{u}_{k-1} &= D^\dagger C \zeta_k - D^\dagger(y_k - CA^k x_0), \quad k = 1, \dots, l, \end{aligned} \quad (16)$$

where $x_0 = C^{-1}y_0$ and the intermediate variable $\zeta_0 = 0$. Then with $\hat{u}_{0:l-1}$, we have

$$\eta_{k+1} = A\eta_k + AB\hat{u}_k, \quad \hat{x}_k = -\eta_k - B\hat{u}_k + A^k x_0, \quad (17)$$

where the intermediate variable $\eta_0 = 0$. We omit the subscript here for brevity, i.e., $\hat{u}_k = \hat{u}_{k|l}$ and $\hat{x}_k = \hat{x}_{k|l}$.

Then, from Lemma 3, it is obvious to find that sequence pairs $(\bar{\mathcal{Y}}^j, \mathcal{X}^j), j = 1, \dots, M$ share the same $\{A_{0:l-1}^c\}$. Therefore, similar as the infinite time case, for each k , we design the estimator as

$$\hat{A}_k^c = C^{-1}(Y_k X_k^T)(X_k X_k^T)^{-1}, \quad (18)$$

where $X_k = (\hat{x}_k^1, \dots, \hat{x}_k^M)^T$ and $Y_k = (\bar{y}_{k+1}^1, \dots, \bar{y}_{k+1}^M)^T$. The matrix $X_k^T X_k$ is required to be full rank ($M \geq n$) to guarantee the uniqueness. Then we have

$$\hat{K}_k = B^\dagger(A - \hat{A}_k^c), \quad k = 0, \dots, l-1, \quad (19)$$

and $\lim_{l \rightarrow \infty} \|\hat{K}_k - K_k\| = 0$ [38].

• Objective Function Parameter Calculation

After obtaining the feedback gain matrix estimation sequence $\hat{K}_{0:l-1}$, we now find a parameter set (H, Q, R) that generates $\hat{K}_{0:l-1}$ exactly through iteration equations (13), (14). Similarly, we provide the following theorem first to show the scalar ambiguity property under this case.

Theorem 3. Suppose two feedback gain matrix sequences $K_{0:N-1}, K'_{0:N-1}$ are generated with two sets of parameters H, Q, R and H', Q', R' respectively through equation (13). If there exist at least $\frac{mn(n+1)(m+1)}{2}$ linearly independent $\text{vec}(\mathcal{P}_i(\mathcal{E}_i))$ defined in (45) and $K_k = K'_k$ for all k , we have $H' = \alpha H, Q' = \alpha Q, R' = \alpha R$ for some $\alpha \in \mathbb{R}_+$.

Proof. See the proof in Appendix D. \square

Corollary 1. Theorem 3 provide a criteria for the identifiability of the objective function. If the control horizon is set as $N < \frac{mn(n+1)(m+1)}{2}$, the true weight parameters H, Q, R of the control objective will never be identified accurately, which can be utilized in preserving the system's intention.

Now, with the identifiability guarantee, we introduce our IOC algorithm based on following lemma derived from (13).

Lemma 4. For H, Q, R in the objective function J_0 , we have

$$a_i(I_i \otimes R)b_i = c_i \begin{bmatrix} H & 0 \\ 0 & I_{i-1} \otimes Q \end{bmatrix} d_i, \quad (20)$$

for $i = 1, \dots, T$ and

$$\begin{aligned}
a_i &= [I_n \quad -B^T K_{N-i+1}^T \quad -B^T A_{N-i+1}^c K_{N-i+2}^T \quad \dots \\
&\quad -B^T \prod_{r=2}^{i-1} A_{N-r}^c K_{N-1}^T], \\
c_i &= B^T [\prod_{r=1}^{i-1} A_{N-r}^c \quad \prod_{r=2}^{i-1} A_{N-r}^c \quad \dots \quad A_{N-i+1}^c \quad I_n], \\
b_i &= \begin{bmatrix} K_{N-i} \\ K_{N-i+1} A_{N-i}^c \\ \vdots \\ K_{N-1} \prod_{r=2}^i A_{N-r}^c \end{bmatrix}, \quad d_i = \begin{bmatrix} \prod_{r=1}^i A_{N-r}^c \\ \prod_{r=2}^i A_{N-r}^c \\ \vdots \\ A_{N-i}^c \end{bmatrix},
\end{aligned} \tag{21}$$

where $K_{N-T:N-1}$ are gain matrices.

Proof. See the proof in Appendix E. \square

Note that equation (20) iterates from $k = N - 1$, which is the reason why we require the observations to contain the final state of trajectories in the previous step.

Set (20) as the constraint of our estimation problem and Theorem 3 ensures the identifiability of H, Q, R (i.e., as the observations increase, the estimation error of \hat{K}_k decreases and we obtain the real parameters), while we use an additional criteria to guarantee the uniqueness of the solution that estimates must minimize the condition number of the block diagonal matrix consisting of $\hat{H}, \hat{Q}, \hat{R}$. Supposing we obtain $\hat{K}_{N-T:N-1}$, the optimization problem is formulated as:

Problem 2. (H, Q, R Estimation with Condition Number Minimization)

$$\begin{aligned}
(\hat{H}, \hat{Q}, \hat{R}, \hat{\tau}) &= \arg \min_{H, Q, R, \tau} \tau^2 \\
\text{s.t.} \quad (20), \quad I &\preceq \text{diag}(H, Q, R) \preceq \tau I.
\end{aligned} \tag{22}$$

For Problem 2, the number of equality constraints and $T \leq N$ in (20) can be decided by the trade-off between accuracy and computation cost. If the gain matrix estimations are all accurate, the above LMI problem is feasible. Since it is a convex optimization problem with linear constraints, there exists at least one exact solution. However, due to the existence of observation noises, the estimation may contain errors and the problem has no solution (infeasible). Therefore, We offer a further analysis to determine whether Problem 2 is solvable. Write formula (20) into following expression:

$$\underbrace{(b_i^T \otimes a_i) \cdot \text{vec}(I_i \otimes R)}_{\mathcal{G}^1(R)} = \underbrace{(d_i^T \otimes c_i) \cdot \text{vec}\left(\begin{bmatrix} H & 0 \\ 0 & I_{i-1} \otimes Q \end{bmatrix}\right)}_{\mathcal{G}^2(H, Q)},$$

for $i = 1, \dots, T$. Define the rows of zero element in the vector $\mathcal{G}^1(R)$ as set \mathcal{C}^1 , $\mathcal{C}^1 = \{k | \mathcal{G}^1(R)_k = 0\}$ and set \mathcal{C}^2 for $\mathcal{G}^2(H, Q)$ similarly. Then we take

$$\mathcal{K}_i^1 = (b_i^T \otimes a_i)(:, \mathcal{C}^1), \quad \mathcal{K}_i^2 = (d_i^T \otimes c_i)(:, \mathcal{C}^2),$$

with which (20) is simplified into

$$\mathcal{K}_i^1 \cdot (\mathbf{1}_i \otimes \text{vec}(R)) = \mathcal{K}_i^2 \cdot \begin{bmatrix} \text{vec}(H) \\ \mathbf{1}_{i-1} \otimes \text{vec}(Q) \end{bmatrix} \tag{23}$$

Therefore, we can combine all the T equations as

$$\begin{aligned}
\tilde{\mathcal{K}}_T^1 \cdot (\mathbf{1}_T \otimes \text{vec}(R)) &= \tilde{\mathcal{K}}_T^2 \cdot \begin{bmatrix} \text{vec}(H) \\ \mathbf{1}_{T-1} \otimes \text{vec}(Q) \end{bmatrix} \\
\Leftrightarrow \underbrace{[\tilde{\mathcal{K}}_T^1 \quad -\tilde{\mathcal{K}}_T^2]}_{\Phi_T} \cdot \underbrace{\begin{bmatrix} \mathbf{1}_T \otimes \text{vec}(R) \\ \text{vec}(H) \\ \mathbf{1}_{T-1} \otimes \text{vec}(Q) \end{bmatrix}}_{\Theta_T(H, Q, R)} &= \begin{bmatrix} 0 \\ \vdots \\ 0 \end{bmatrix},
\end{aligned} \tag{24}$$

where

$$\tilde{\mathcal{K}}_T^1 = \begin{bmatrix} \mathcal{K}_1^1 & 0 & \dots & 0 \\ \mathcal{K}_2^1 & \dots & \dots & 0 \\ \vdots & \vdots & \vdots & \vdots \\ \mathcal{K}_T^1 & & & \end{bmatrix}, \quad \tilde{\mathcal{K}}_T^2 = \begin{bmatrix} \mathcal{K}_1^2 & 0 & \dots & 0 \\ \mathcal{K}_2^2 & \dots & \dots & 0 \\ \vdots & \vdots & \vdots & \vdots \\ \mathcal{K}_T^2 & & & \end{bmatrix}.$$

Based on the above derivation, we provide the following theorem.

Theorem 4. *Problem 2 is infeasible, when the rank*

$$\text{rank}(\Phi_T) \geq n^2 + n + \frac{m^2 + m}{2}, \tag{25}$$

which implies that the equation

$$\Phi_T \cdot \Theta_T(X_h, X_q, X_r) = \mathbf{0}$$

has only zero solution for unknown variables $X_h, X_r \in \mathbb{S}^n$ and $X_q \in \mathbb{S}^m$.

Therefore, we consider the following optimization problem instead when Problem 2 is infeasible:

$$\begin{aligned}
\min_{\hat{H}, \hat{Q}, \hat{R}} \quad & \|\Phi_T \cdot \Theta_T(\hat{H}, \hat{Q}, \hat{R})\|_2^2 \\
\text{s.t.} \quad & \|\Theta_T(\hat{H}, \hat{Q}, \hat{R})\| = 1,
\end{aligned} \tag{26}$$

which can be solved by existing QP solvers [39].

IV. CONTROL HORIZON ESTIMATION AND LQR PROBLEM RECONSTRUCTION

Note that with the target state and objective function, we can generate a satisfying control trajectory. However, in order to imitate the agent's motion precisely, we still need to estimate the control horizon, since different control horizons lead to different inputs and final states.

In this section, we will first introduce the control horizon estimation algorithm, then reconstruct the LQR problem with estimates and provide the input prediction application.

A. Control Horizon Estimation

Suppose R_m is now driving under an optimal trajectory generated by \mathbf{P}_0 toward the target. To estimate the control horizon N of this trajectory, we need an l length continuous observation

$$\mathcal{Y} = \{y_0, y_1, \dots, y_l\}. \tag{27}$$

We build the following optimization problem for estimation.

Problem 3. (Estimation of the Control Horizon)

$$\begin{aligned}
\min_{\hat{N}} \quad & \sum_{i=1}^l \|y_i - Cx_i\|^2 := J_N(\hat{N}; y_{0:l}) \\
\text{s.t.} \quad & x_{k+1} = Ax_k + Bu_k, \\
& u_i = -K_i x_i, x_0 = y_0 - \hat{x}_T, \\
& K_i = (\hat{R} + B^T P_{i+1} B)^{-1} B^T P_{i+1} A, \\
& P_i = K_i^T \hat{R} K_i + A_i^{cT} P_{i+1} A_i^c + \hat{Q}, P_{\hat{N}} = \hat{H}, \\
& i = 0, 1, \dots, \hat{N} - 1,
\end{aligned}$$

where $y_{1:l}$ is the observation of R_m up to time $k = l$.

The above problem reflects that the deviation of the trajectory obtained under the optimal solution \hat{N}^* from the observed data $y_{1:l}$ is the smallest. Since the optimization variable $\hat{N} \in \mathbb{N}_+$ does not explicitly exist in the objective and constraints, the problem is a non-convex optimization on the set of positive integers and hard to solve directly. Therefore, we turn to investigate how the value of the objective function changes with \hat{N} . Note that $N > l$ and as \hat{N} grows from l to the real horizon N , the function J_N gradually decreases to the minimum point. Then, as the continue growth of \hat{N} , J_N increases and finally converges to a fixed value $\sum_{i=1}^l \|y_i\|^2$. See an illustration in Fig. 4 of Section V.

According to the analysis of J_N , to obtain the solution of Problem 3, we can start traversing from $\hat{N} = l$ and keep increasing \hat{N} until J_N no longer decreases, at which time the optimal \hat{N}^* is found. However, this will consume lots of computation if $N \gg l$. Therefore, we propose an algorithm based on binary search to find the optimal solution inspired by the line search of gradient decent method. Since J_N is a discrete function with respect to \hat{N} , we use the function values at both \hat{N} and $\hat{N} + 1$ to approximate the gradient at point \hat{N} , which is given by:

$$g_N = \frac{J_N(\hat{N} + 1; y_{0:l}) - J_N(\hat{N}; y_{0:l})}{(\hat{N} + 1) - \hat{N}}. \quad (29)$$

Thus, if we have $g_N < 0$, then $\hat{N} < \hat{N}^*$; if $g_N > 0$, then $\hat{N} \geq \hat{N}^*$. The detailed algorithm is shown in Algorithm 1.

Remark 3. Notice that after determining the initial range $[N^-, N^+]$, if we simply leverage the function values of the two break points $N_1, N_2, N^- \leq N_1 < N_2 \leq N^+$ to find the optimum, to have a constant compressive ratio c , the break points should satisfy $\frac{N_2 - N^-}{N^+ - N^-} = \frac{N^+ - N_1}{N^+ - N^-} = c$ and $c = \frac{\sqrt{5}-1}{2} \approx 0.618$. However, with the above Algorithm 1, since we approximate the gradient, the compressive ratio is improved to $c = 0.5$. Moreover, in order to reduce the computation cost, it is recommended to store the result each time we calculate the deviation sum J_N corresponding to a certain \hat{N} to avoid repeated calculation.

B. LQR Reconstruction

Now we have obtained the estimate of the target state \hat{x}_T , the control horizon \hat{N}^* , and identified the weighting matrices in objective function J_0 . Therefore, we can reconstruct the

Algorithm 1: Binary Search for Optimal \hat{N}

Input: The observation trajectory and the observation times, $y_{0:l}, l$; The estimate of the target state, \hat{x}_T ; The parameters of the system dynamic, A, B, C ; The estimate of the objective function parameter, $\hat{H}, \hat{Q}, \hat{R}$; The step length, θ ;

Output: The optimal control horizon estimate, \hat{N}^* ;

Determine the initial bound:
Set the lower bound as $N^- = l + 1$; Let $\hat{N}' = l + \theta$;
while $g_{\hat{N}'} < 0$ **do** $\hat{N}' = \hat{N}' + \theta$; ;
Set the upper bound as $N^+ = \hat{N}'$;

Binary search:
Take the midpoint of the range as $\tilde{N} = \lfloor \frac{N^- + N^+}{2} \rfloor$;
while $N^+ - N^- > 1$ **do**
 if $g_{\tilde{N}} > 0$ **then** Set $N^+ = \tilde{N}$;
 else Set $N^- = \tilde{N}$;
end
 $\hat{N}^* = \arg \min_{\hat{N}} \{J_N(\hat{N}; y_{0:l}); \hat{N} \in \{N^+, N^-\}\}$;

return The control horizon estimation \hat{N}^* .

optimization problem by substituting x_T, H, Q, R, N in \mathbf{P}_0 with our estimates and calculate the control law $\hat{K}_{0:\hat{N}-1}$ through the iteration (13) and (14).

We provide the future input prediction as one important application of our control law learning algorithm. Now suppose at time $k = l$, the agent R_o has observed R_m for $l + 1$ steps and obtained a series of observations \mathcal{Y} as (27). Denote u_l as the real input at $k = l$ that we want to predict and $\hat{u}_{l|l}$ as our input inference. R_o tries to infer the current control input accurately, which is to minimize the error between $\hat{u}_{l|l}$ and u_l . From (5), u_l is calculated by $-K_l x_l$, then we have

$$\min \|u_l - \hat{u}_{l|l}\|^2 = \|-K_l x_l - \hat{u}_{l|l}\|^2, \quad (30)$$

Notice that the state estimate $\hat{x}_{l|l}$ can be obtained by Kalman filter. Therefore, we can infer the control input of the target agent R_m at time l by

$$\hat{u}_{l|l} = \mu_0, \quad (31)$$

where μ_0 is calculated by solving the following reconstructed optimization problem:

Problem 4. (Control Input Prediction)

$$\begin{aligned}
\min_{\mu_{0:N'-1}} \quad & J' = x_{N'}^T \hat{H} x_{N'} + \sum_{k=0}^{N'-1} (x_k^T \hat{Q} x_k + \mu_k^T \hat{R} \mu_k) \\
\text{s.t.} \quad & (1), x_0 = \hat{x}_{l|l} - \hat{x}_T,
\end{aligned}$$

in which $N' = \hat{N}^* - l$.

The solution of this reconstructed LQR problem is given in [40] as

$$\mu_0 = -K_0 x_0, \quad (32)$$

where K_0 is calculated by (13).

Remark 4. According to the principle of optimality [41] in the dynamic programming, if a control policy $p_{0,N}^*$ is optimal for the initial point x_0 , then for any $l \in \{1, 2, \dots, N-1\}$, its sub-policy $p_{l,N}^*$ is also optimal to the subprocess containing last $N-l+1$ steps with the initial point x_l .

• Prediction Error Analysis

Note that when the trajectory sample size $M \rightarrow \infty$, we have $\hat{x}_T = x_T$ and $\hat{H} = H, \hat{R} = R, \hat{Q} = Q$ according to the law of large numbers. However, the accuracy of estimation \hat{N}^* can not be guaranteed, since it is the value that minimize function J_N , which is affected by the observation errors. Therefore, the sensitivity of \hat{N}^* with respect to the input estimation $\hat{u}_{l|l}$ needs to be analyzed.

It is found that the influence of \hat{N}^* is reflected in the calculation of K_0 with Problem 4 and formula (33). Now suppose the real control horizon of the system N generates K_0^r , while our estimate \hat{N}^* calculates \hat{K}_0 . We will show the estimation error $\|\hat{K}_0 - K_0^r\|$ can be bounded and controlled in the following analysis.

Note that a discrete-time LQR problem with finite control horizon as \mathbf{P}_0 is solved through dynamic programming method and the iteration equation of the intermediate parameter P_k can be described as

$$P_{k-1} = A^T P_k A - A^T P_k B (R + B^T P_k B)^{-1} B^T P_k A + Q,$$

for $k = 1, \dots, N$ with $P_N = H > 0$. According to [42], when $N \rightarrow \infty$, there is $P_0 = P^* > 0$, where P^* satisfies the discrete Riccati equation:

$$P^* = A^T P^* A - A^T P^* B (R + B^T P^* B)^{-1} B^T P^* A + Q, \quad (34)$$

and correspondingly,

$$K_0 = K^* = (R + B^T P^* B)^{-1} B^T P^* A.$$

What's more, the sequence $\{P_k\}$ is monotonic (In our analysis, a matrix sequence is monotonic means $P_0 \preceq P_1 \preceq \dots \preceq P_N$, where $P_i \geq P_j$ implies $P_i - P_j$ is a positive semi-definite matrix). According to Lemma 3, the difference between the ends of two trajectories with control horizons $N_1, N_2, N_1 \leq N_2$ can be converted to a comparison inside a single sequence generated by N_2 , which is $\|K_0^{(1)} - K_0^{(2)}\| = \|K_{N_2-N_1}^{(2)} - K_0^{(2)}\|$. Therefore, we have the estimation error

$$\|\hat{K}_0 - K_0^r\| = \|K_{|\hat{N}^* - N|} - K_0\|,$$

where $K_{0:N_m}$ is generated under the horizon $N_m = \max(N, \hat{N}^*)$. Then we will focus on the convergence of the $\{K_k\}$ sequence under fixed H, Q, R .

We offer the following theorem to show the input prediction error and sensitivity of the control horizon estimate.

Theorem 5. There exists a positive integer $\bar{N} \in \mathbb{N}_+$ and $\eta > 0$, which can be set as the maximum tolerable inference error. For any $N > \bar{N}$, we have $\|\mu_0^{(N+\delta N)} - \mu_0^{(N)}\| \leq \eta$, where $\mu_0^{(N)}$ denotes the input inference when the control horizon estimate $\hat{N}^* = N$ and η is proportional to $\delta N \in \mathbb{N}_+$.

Proof. See the proof in Appendix F. □

The complete algorithm flow is shown in Algorithm 2.

Algorithm 2: LQR Reconstruction based Control Inputs Prediction Algorithm

Input: The observation data including M history trajectories, $\{\mathcal{Y}^{1:M}\}$; The observation of current trajectory and the observation times, \mathcal{Y}, l ; The system dynamic function, A, B, C ;

Output: The control input inference at time l , $\hat{u}_{l|l}$; Estimate the target state \hat{x}_T through curve fitting and calculating the intersection;

if consider only final-state **then**

Identify the objective function parameter \hat{R} by solving Problem 1 with M trajectories;

else if consider process-states **then**

Estimate the feedback gain matrices;

Identify $\hat{H}, \hat{Q}, \hat{R}$ by solving Problem 2;

else Return false;

Calculate the optimal estimate to control horizon \hat{N}^* with Algorithm 1;

Formulate and solve Problem 4 with previous estimates; Obtain the one-step input μ_0 with (33) in the forward pass;

return The control input prediction $\hat{u}_{l|l} = \mu_0$.

V. SIMULATION RESULTS

In this section, we conduct multiple simulations on our algorithm and apply it to the future input and trajectory prediction to show the performance and efficiency.

Consider a controllable linear system modeled by a three-dimensional dynamical function as (1) and

$$A = \begin{bmatrix} 1.4155 & -0.0876 & 0.7213 \\ 0.8186 & 2.7338 & -1.2750 \\ -0.3118 & -0.7573 & 1.2008 \end{bmatrix}, \quad (35)$$

$$B = \begin{bmatrix} -0.0484 & 0.1611 & -1.8972 \\ -1.1350 & 1.6600 & 0.1003 \\ 0.3905 & -0.7851 & 0.1055 \end{bmatrix},$$

are generated randomly where $n = m = 3$. Assume the agent is driving to the target state $[6, 8, 4]^T$. The observation function is (2) with $C = I_3$ and the observation noise satisfies a Gaussian distribution $\mathcal{N}(0, 0.02^2)$. We now obtain a set of trajectory observation. Through applying the external incentives and the line fitting, we calculate the intersection point as the estimation to the target state

$$\hat{x}_T = [6.063, 8.086, 4.039]^T.$$

A. Final-state Only Setting

Firstly, we consider the control optimization problem \mathbf{P}_0 with final-state setting (as J_1). We suppose

$$H = I_{3 \times 3}, R = \begin{bmatrix} 0.4I_{2 \times 2} & 0_{2 \times 1} \\ 0_{1 \times 2} & 0.8 \end{bmatrix}.$$

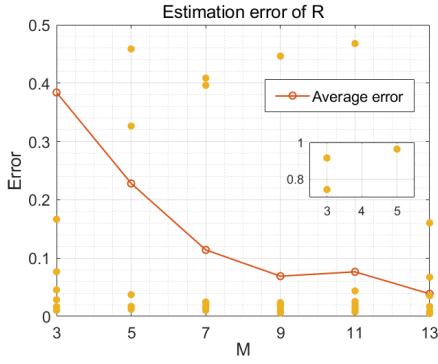


Fig. 2. Estimation results of the parameter R under only final-state setting. We launch the simulation 8 times at each M . The yellow dots are estimation errors of each simulation and the red curve represents the change of the average error from $M = 3$ to 13.

TABLE II
TIME COST OF R ESTIMATION

Amount of Data M	2	4	6	8	10
Time Cost (s)	0.5436	0.7829	1.071	1.431	1.806

To test the estimation algorithm for R , we set the trajectory length $l_j = 10$ and random initial states x_0^j for all $j = 1, 2, \dots, M$ to ensure the linear independence. Use the MATLAB function *fmincon* with “interior-point” method to solve Problem 1. We pick the Frobenius norm to measure the estimation error:

$$err(\hat{R}) = \frac{\|\hat{R} - R\|_F}{\|R\|_F}.$$

The results are shown in Fig. 2 and the time costs are listed in Table.II. Notice that R is a three-dimensional matrix, more than three trajectories are required to solve for a unique \hat{R} . We can see that as the number of trajectories M increases from 3 to 13, the estimation error shows a decreasing trend. However, as M becomes larger, the search space of the problem increases as well and we need to continuously enlarge the parameter *MaxfunEvals* of function *fmincon* to ensure an accurate solution. The larger number of iterations leads to a longer solving time. Therefore, considering the trade-off between the estimation error and the computational efficiency, we choose $M = 7$ and the estimation value

$$\hat{R} = \begin{bmatrix} 0.4193 & -0.0078 & -0.0063 \\ -0.0026 & 0.4083 & -0.0071 \\ -0.0089 & -0.0111 & 0.8166 \end{bmatrix}.$$

B. Classic LQR Setting

Now we consider the more complex objective function setting as J_0 in (12). We set parameters

$$H = I_{3 \times 3}, Q = 0.2I_{3 \times 3}, R = \begin{bmatrix} 0.4I_{2 \times 2} & 0_{2 \times 1} \\ 0_{1 \times 2} & 0.8 \end{bmatrix}$$

and estimate them simultaneously by the algorithm in Sec. III-B. We first collect M trajectories containing their terminal

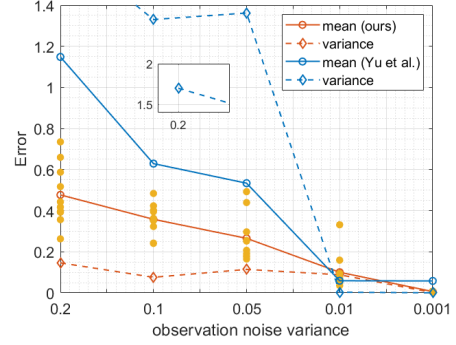


Fig. 3. Estimation results of the parameters H, Q, R . We run experiments for 10 times at different variances of observation noise from 0.2 to 0.001. The red lines show estimation errors of our algorithm with yellow dots representing each simulation results and blue lines are results of method proposed in [21] ($H = Q$), where the solid line is mean of the errors and the dashed line is the standard deviation.

states and compute the feedback matrix K_k at each step using the proposed estimator as (18). Note that when there is no observation noise, Problem 2 is always feasible with any T since $rank(\Phi_T) = 9 < n^2 + n + \frac{m^2+m}{2} = 18$ according to Theorem 4, and the solutions are accurately equal to the real H, Q, R . However, if the observation noise exists, in this case Problem 2 is only feasible at $T = 1$ ($rank(\Phi_1) = 9 < 18$). For $T \geq 2$, we have $rank(\Phi_1) = 9 \cdot T \geq 18$ which needs to transfer into the QP problem as (26).

Here we set $T = 6$ and solve Problem 2 and (26) with solver YALMIP [43] and SeDuMi [44] in MATLAB. The estimation errors are shown in Fig. 3. We use the Frobenius norm to measure the estimation error:

$$err = \frac{\|\begin{bmatrix} \hat{H} & \hat{Q} & \hat{R} \end{bmatrix} - \begin{bmatrix} H & Q & R \end{bmatrix} \cdot \alpha\|_F}{\|\begin{bmatrix} H & Q & R \end{bmatrix} \cdot \alpha\|_F}.$$

With the trajectory number fixed, as observation noises decrease, the estimate to \hat{K}_k becomes more accurate and estimation errors of $\hat{H}, \hat{Q}, \hat{R}$ gradually decrease. We compare with the IOC algorithm proposed in [21] (we set $H = Q$ here since [21] estimates Q, R only) and find that when the observation noise is small enough, the estimation errors obtained by two algorithms are basically the same, while when the noise is not negligible, ours works better. What’s more, comparing the variance of multiple simulation results, our algorithm is overall smaller and more stable than theirs. Finally we take the following estimates:

$$\hat{H} = \begin{bmatrix} 5.0699 & -0.1320 & -0.1507 \\ -0.1320 & 4.9445 & -0.0058 \\ -0.1507 & -0.0058 & 4.9836 \end{bmatrix},$$

$$\hat{Q} = \begin{bmatrix} 1.0069 & 0.0097 & 0.0045 \\ 0.0097 & 1.0137 & 0.0064 \\ 0.0045 & 0.0064 & 1.0030 \end{bmatrix},$$

$$\hat{R} = \begin{bmatrix} 1.9926 & -0.0791 & -0.1309 \\ -0.0791 & 1.9727 & -0.0556 \\ -0.1309 & -0.0556 & 3.8733 \end{bmatrix}$$

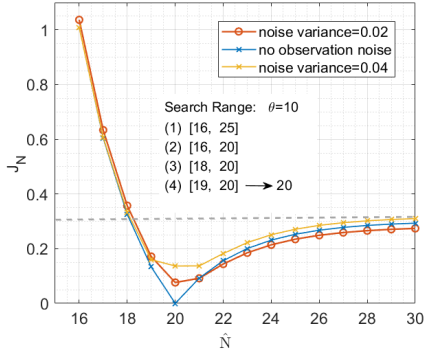


Fig. 4. The function value J_N of different estimation \hat{N} . Set the observation number $l = 15$ and the real control horizon $N = 20$. The red curve shows the change of function J_N with \hat{N} when the observation noise variance equal to 0.02 (our simulation setting). We can see that J_N decreases at the beginning and reaches the minimum value at 20. Then it gradually increases and converges to $\sum_{i=1}^{15} \|y_i\|^2$. Note that as the noise variance goes larger, the minimum point of J_N may deviate from 20 as the yellow curve and Theorem 5 is proposed for analyzing the error's bound.

TABLE III
STATES PREDICTION ERROR COMPARISON

Step k	16	17	18	19	20
Ours	0.0365	0.0271	0.0184	0.0106	0.0048
[26]	0.0543	0.1105	0.2006	0.3378	0.5401

with the multiplied scalar $\alpha = 5$.

Now we start to infer the inputs and predict the future states of the agent. Observe for $l = 15$ times and set $\theta = 10$. With Algorithm 1 and the property of J_N curve in Fig. 4, we obtain the optimal control horizon estimation $\hat{N}^* = 20$. At this point, we have completed the estimation of \hat{x}_T , \hat{R} and \hat{N}^* . The current state is estimated by Kalman filter as $\hat{x}_{l|l}$. Then, we reconstruct and solve the control optimization problem of the mobile agent as Problem 4:

$$\begin{aligned} \min_{\mu_{0:4}} \quad & x_5^T \hat{H} x_5 + \sum_{k=0}^4 (\mu_k^T \hat{R} \mu_k + x_k^T \hat{Q} x_k) \\ \text{s.t.} \quad & (1), x_0 = \hat{x}_{l|l} - \hat{x}_T, k = 0, \dots, 4. \end{aligned}$$

Note that the solution $x_{1:5}$ of above problem are actually the prediction to the future state of the agent from $k = 16$ to 20. Denote the prediction error as $\|\hat{x} - x\|$. Comparing with the prediction through polynomial regression [26] in presence of the same observation noise distribution, the results are shown in Table.III. The curve fitting is based on all the $l = 15$ history states and the highest polynomial order is chosen as 3 which is the optimal. We can see that the prediction error generated by our methods is overall lower than the fitting methods. Moreover, the error by curve fitting grows larger with time k while the error of our method decreases as x_k goes to 0.

VI. EXPERIMENTS

We demonstrate the algorithm on our self-designed mobile robot platform [45] as Fig. 5. The AprilTag visual system is

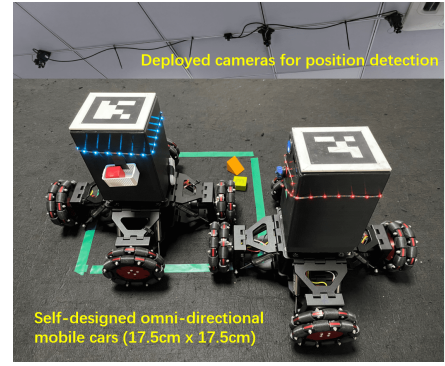


Fig. 5. The self-designed platform. Each omni-directional mobile agent has a unique QR code on its top for the position detection. A high-precision camera array is deployed on the ceiling.

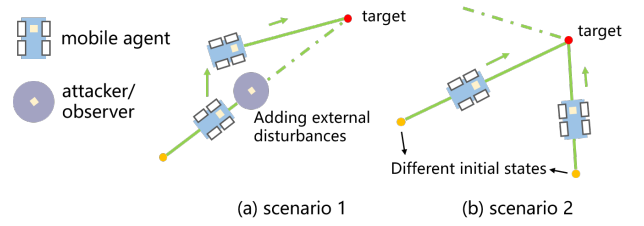


Fig. 6. Two scenarios of data collection process. Scenario 1 leverages the mechanism that the agent will re-calculate the trajectory after receiving disturbances, while scenario 2 just observes and records different trajectories from different initial point.

adopted for the real-time localization of the robots. The control procedures based on the localization results are implemented by MATLAB in a VMWare ESXI virtual machine, which is equipped with an Intel(R) Xeon(R) Gold 5220R CPU, 2.20G Hz processor and 16GB RAM. All experiments are conducted on a $5\text{m} \times 3\text{m}$ square platform, and two $17.5\text{cm} \times 17.5\text{cm} \times 20\text{cm}$ omni-directional mobile cars are used.

We simulate a carrying scenario. A moving agent equipped with the blue light strip transports building blocks from different locations to the green box under LQR optimal control, while the car with red lights acts as an external attacker to observe and record the trajectory of the blue one in order to reconstruct its optimization problem, thereby inferring the future state or imitating its behavior. We have the system state $x_k = (x_k^x \ x_k^y)^T$ and input vector $u_k = (u_k^x \ u_k^y)^T$, where the superscript indicates the horizontal or vertical direction. The control problem of the moving agent is described as \mathbf{P}_0 with $A = C = I_2, B = 0.2I_2$ and $N = 15, H = 5I_2, Q = 0.1I_2, R = 0.5I_2$. Set $x_T = (3000, 2000)^T$ as the target state.

During the data collection period, two kinds of conditions described in Fig. 6 are considered. Notice that in scenario 1, R_m will re-calculate its trajectory after being disturbed. Therefore, we can leverage this mechanism and actively apply external inputs to collect multiple different trajectories. Referring to Fig. 7(a)-(d), the moving agent starts from three initial points including $[1430, 1457], [2196, 1185], [1738, 2389]$

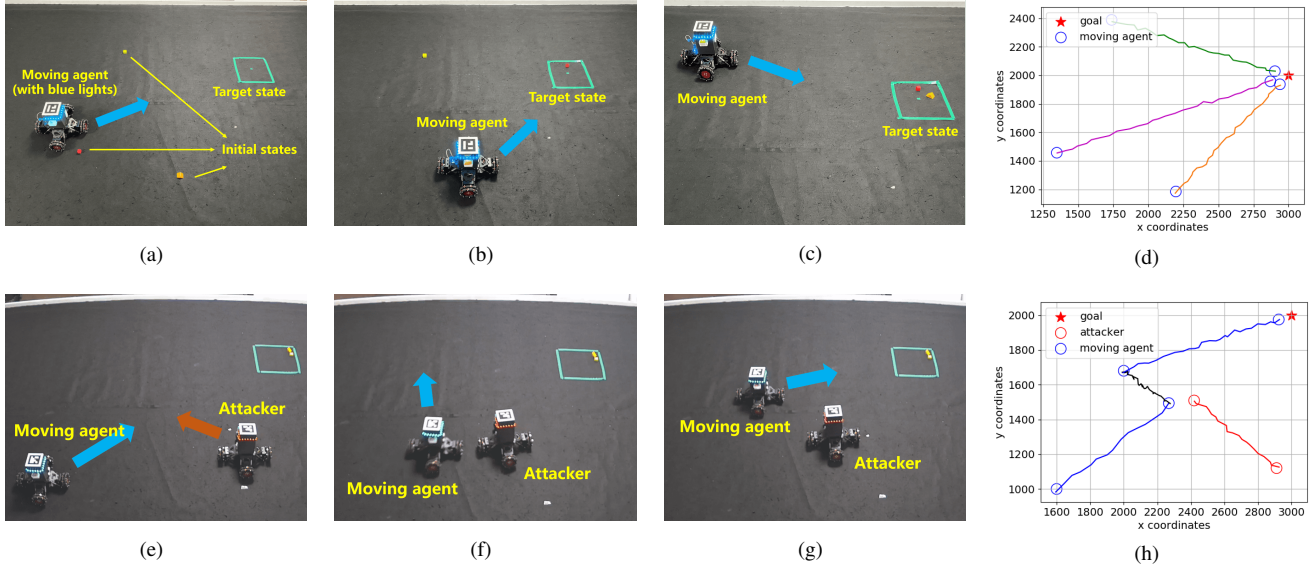


Fig. 7. The illustration of data collection process. The green square is the target state and the moving agent with blue lights drives to the target from different initial position, being observed by the attacker with red lights, which provides multiple unparallelled trajectory observations.

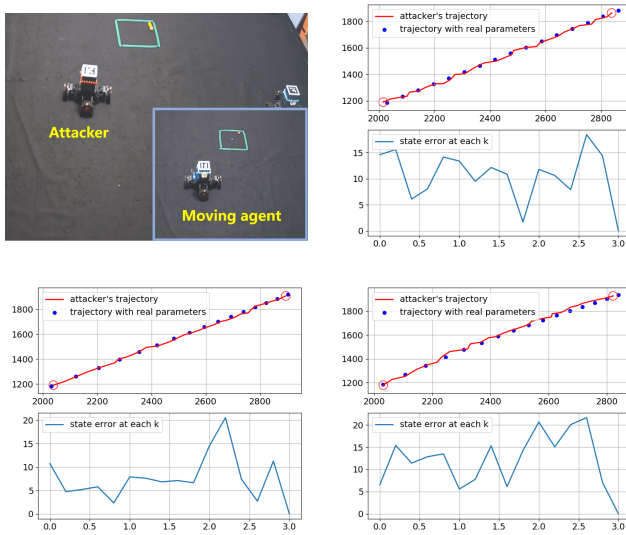


Fig. 8. The attacker learns the control law and imitates trajectories of the moving agent under different motions including uniform linear, variable speed linear and variable speed curve motion.

in sequence and drives to the set target, which provides three unparallelled trajectory observations. Another situation is shown as Fig. 7(e)-(h) which leverages the attacker as an external stimulate and makes the agent to re-plan from its current state, leading to two different trajectories. Therefore, we take four trajectories as observation data and launch our algorithm. We have $\hat{x}_T = (2973.3, 1989)^T$ and the estimation

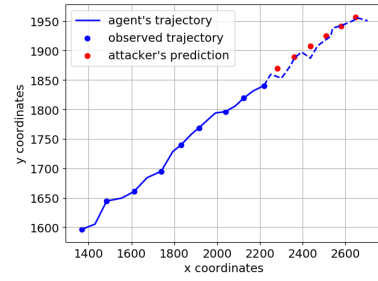


Fig. 9. Conduct the LQR reconstruction based input prediction algorithm on the self-designed platform. The blue line (and the dash line) is the agent's real trajectory. The blue scatters are observed states sequence and the red are our future state prediction.

results of objective function parameters are

$$\hat{H} = \begin{bmatrix} 49.0753 & -2.1655 \\ -2.1655 & 48.6586 \end{bmatrix}, \hat{Q} = \begin{bmatrix} 1.0025 & -0.0060 \\ -0.0060 & 1.0143 \end{bmatrix},$$

$$\hat{R} = \begin{bmatrix} 4.8863 & -0.2250 \\ -0.2250 & 4.8459 \end{bmatrix}.$$

When the attacker successfully reconstructs the control optimization problem with the estimates of all the parameters, we demonstrate that starting from an arbitrary starting point, the attacker can mimic the trajectories of the agent under different motions and accurately predict the future state with Algorithm 2 as shown in Fig. 8 and 9 respectively. All experiments demonstrate the effectiveness of the proposed reconstruction algorithm. More tests including variable speed and curve motions can be found in the video <https://youtu.be/rUWd9k3-mg>.

VII. CONCLUSION

This paper proposes an algorithm for learning the control law of a moving agent under LQR control with optimization

problem reconstruction based on observations. Assuming the linear dynamical system and the quadratic objective function form is known, we identify the parameters in the objective function based on inverse optimal control considering of settings and estimate the control horizon with a binary search method. Finally, we reconstruct the control optimization problem of the agent and calculate its solution as the learned control law. We apply our algorithm to predict the future input and conduct extensive simulations and hardware experiments to demonstrate its efficiency. Future work may consider non-linear modeled agents and identifying more complex objective functions with constraints and obstacles in the environment.

APPENDIX A PROOF OF LEMMA 2

Apply the problem constraints to the new parameters H', R' . We obtain that $(\lambda_i^j)' = \alpha \lambda_i^j$ for all i, j and

$$\begin{aligned} (x_{i+1}^j)' &= A(x_i^j)' - B(R')^{-1}B^T(\lambda_{i+1}^j)' \\ &= A(x_i^j)' - BR^{-1}B^T\lambda_{i+1}^j. \end{aligned}$$

Comparing to $x_{i+1}^j = Ax_i^j - BR^{-1}B^T\lambda_{i+1}^j$, if we have $(x_0^j)' = x_0^j$, it is easy to realize that $H', R', x_{1:N}^j, (\lambda_{1:N}^j)'$ are also solutions to the problem with the same objective function value of the real parameters H, R .

APPENDIX B PROOF OF THEOREM 1

Now we will show that if A_k^c and $A_k^{c'}$ defined in the theorem are equal for all k , then we have $R = R'$. We prove this by contradiction. Suppose the two corresponding positive definite matrices R, R' are different, then define

$$\Delta R = R' - R \neq 0,$$

where ΔR is also a symmetric matrix. Then there are two sets of matrices $P_{0:N}, K_{0:N-1}$ and $P'_{0:N}, K'_{0:N-1}$ satisfying the iteration equations:

$$K_k = (R + B^T P_{k+1} B)^{-1} B^T P_{k+1} A, \quad (36)$$

$$P_k = K_k^T R K_k + A_k^{cT} P_{k+1} A_k^c, \quad (37)$$

with $P_N = H = I$ respectively. Since we have $A_k^c = A_k^{c'}$ for all k , there is

$$A - BK_k = A - BK_k' \Leftrightarrow BK_k = BK_k' \Leftrightarrow B^T BK_k = B^T BK_k'.$$

Note that B has full column rank, thus $B^T B$ is invertible. Therefore, we derive $K_k = K_k'$ directly.

According to (36), it follows that

$$\begin{aligned} (R + B^T P_{k+1} B) K_k &= B^T P_{k+1} A, \\ R K_k &= B^T P_{k+1} A_k^c. \end{aligned}$$

Then we also have the above equation for R' and P'_{k+1} which is written as

$$\begin{aligned} (R + \Delta R) K_k &= B^T (P_{k+1} + \Delta P_{k+1}) A_k^c, \\ \Delta R K_k &= B^T \Delta P_{k+1} A_k^c, \end{aligned} \quad (38)$$

where $\Delta P_k = P'_k - P_k$. Similarly, for equation (37) we have

$$\begin{aligned} P_k + \Delta P_k &= K_k^T (R + \Delta R) K_k + A_k^{cT} (P_{k+1} + \Delta P_{k+1} A_k^c), \\ \Delta P_k &= (K_k^T B^T + A_k^{cT}) \Delta P_{k+1} A_k^c. \end{aligned} \quad (39)$$

Since $P_N = P'_N = I$, then $\Delta P_N = 0$. Combining with (39), we have $\Delta P_k = 0$ and $P_k = P'_k$ for all k . Thus (38) converts into

$$\Delta R K_k = 0, k = 0, 1, \dots, N-1.$$

Note that $I \succ 0, R \succ 0$, then with (37) we can obtain that $P_k \succ 0$ and is invertible. Therefore, since P_k, A are all invertible matrices, from (36) we derive $\text{rank}(K_k) = \text{rank}(B^T) = m$. Thus K_k has full row rank and $\Delta R = 0$, which is contradict with the assumption. The proof is done.

APPENDIX C PROOF OF THEOREM 2

Denote $z_i = \begin{bmatrix} x_i^T & \lambda_i^T \end{bmatrix}, i = 1, \dots, N$. Then the constraints for each step in Problem 1 is written as

$$\underbrace{\begin{bmatrix} I & BR^{-1}B^T \\ 0 & A^T \end{bmatrix}}_E z_{i+1} = \underbrace{\begin{bmatrix} A & 0 \\ 0 & I \end{bmatrix}}_F z_i. \quad (40)$$

Combine all the constraints into a matrix equation as follows

$$\underbrace{\begin{bmatrix} \tilde{E} & & \tilde{F} \\ -F & E & \\ & \ddots & \ddots \\ & & -F & E \end{bmatrix}}_{\mathcal{F}(R)} \underbrace{\begin{bmatrix} z_1 \\ z_2 \\ \vdots \\ z_N \end{bmatrix}}_Z = \underbrace{\begin{bmatrix} A \\ 0 \\ \vdots \\ 0 \end{bmatrix}}_{\tilde{A}} x_0, \quad (41)$$

where $\tilde{E} = \begin{bmatrix} I & BR^{-1}B^T \\ 0 & 0 \end{bmatrix}$ and $\tilde{F} = \begin{bmatrix} 0 & 0 \\ -I & I \end{bmatrix}$. Note that $\mathcal{F}(R)$ is an invertible matrix. Then we have

$$\sum_{i=1}^N \|y_i - x_i^*\|^2 = \|Y - G_X Z\|^2 = \|Y - G_X \mathcal{F}(R)^{-1} \tilde{A} x_0\|^2,$$

where $G_X = I_{N-1} \otimes [I_n, 0_n]$. Then the subsequent proof is similar to the proof of Theorem 4.1 in [22]. Just replace $\mathcal{F}(Q)$ in [22] with $\mathcal{F}(R)$ in (41) and we have $\hat{R} \xrightarrow{P} R$ as $M \rightarrow \infty$, where \hat{R} is the solution obtained by Problem 1 and R is the true parameter in the forward problem.

APPENDIX D PROOF OF THEOREM 3

This proof will show that the matrix pairs H, Q, R and H', Q', R' obtained through the iteration equations (13) with same sequence $K_{0:N-1}$ satisfy a scalar multiple relationship under some linearly independent conditions.

From (13) we have

$$\begin{aligned} A_k^c &= A - BK_k = A - B(R + B^T P_{k+1} B)^{-1} B^T P_{k+1} A \\ &= (I + BR^{-1}B^T P_{k+1})^{-1} A, \end{aligned}$$

where we used the Sherman–Morrison formula. Since $K_{0:N-1}$ and $K'_{0:N-1}$ are the same, A_k^c 's corresponding to K_k and K'_k are the same and we have

$$R^{-1}B^T P_{k+1} = R'^{-1}B^T P'_{k+1} \quad (42)$$

for all k , where we used that A is invertible and B has full column rank. For P_k , we have

$$\begin{aligned} P_{k-1} &= A^T P_k A - A^T P_k B (R + B^T P_k B)^{-1} B^T P_k A + Q \\ &= A^T P_k A_{k-1}^c + Q. \end{aligned}$$

Starting from $k = N$ with $P_N = H, P'_N = H'$, we substitute P_k into (42) and obtain the following N equations.

$$\begin{aligned} R^{-1}B^T H &= R'^{-1}B^T H', \\ R^{-1}B^T (Q + A^T H A_{N-1}^c) &= R'^{-1}B^T (Q' + A^T H' A_{N-1}^c), \\ R^{-1}B^T (Q + A^T Q A_{N-2}^c + (A^T)^2 H A_{N-1}^c A_{N-2}^c) &= \\ R'^{-1}B^T (Q' + A^T Q' A_{N-2}^c + (A^T)^2 H' A_{N-1}^c A_{N-2}^c), \\ \dots \end{aligned}$$

In particular, for $k = i$, we have $R^{-1}B^T P_i = R'^{-1}B^T P'_i$, where

$$P_i = Q + \sum_{j=1}^{N-i} (A^T)^j Q \Pi_{r=i}^{i+j-1} A_r^c + (A^T)^{N-i} H \Pi_{r=i}^{N-1} A_r^c.$$

We subtract the equation for $k = i + 1$ from the equation for $k = i$ and write the difference in the following matrix form:

$$R^{-1} \widetilde{\mathcal{B}} \widetilde{\mathcal{A}}_i \widetilde{Q} \widetilde{H}_i \widetilde{\mathcal{A}}_i^c = R'^{-1} \widetilde{\mathcal{B}} \widetilde{\mathcal{A}}_i \widetilde{Q}' \widetilde{H}'_i \widetilde{\mathcal{A}}_i^c, \quad (43)$$

where

$$\begin{aligned} \widetilde{\mathcal{B}} \widetilde{\mathcal{A}}_i &= B^T [A^T, \dots, (A^T)^{N-i-1}, (A^T)^{N-i-1}, (A^T)^{N-i}], \\ \widetilde{\mathcal{A}}_i^c &= [(A_i^c - A_{i+1}^c)^T, \dots, (\Pi_{r=0}^{p-1} A_{i+r}^c - \Pi_{r=1}^p A_{i+r}^c)^T, \dots, \\ &\quad (\Pi_{r=0}^{N-1} A_{i+r}^c)^T, -(\Pi_{r=1}^N A_{i+r}^c)^T, (\Pi_{r=0}^N A_{i+r}^c)^T]^T, \\ \widetilde{Q} \widetilde{H}_i &= \begin{bmatrix} I_{N-i-1} \otimes Q & 0 \\ 0 & I_2 \otimes H \end{bmatrix}. \end{aligned}$$

$\widetilde{Q}' \widetilde{H}'_i$ can be obtained by replacing Q, H in $\widetilde{Q} \widetilde{H}_i$ with Q', H' . Index p in the block matrix $\widetilde{\mathcal{A}}_i^c$ refers to the p -th block, i.e. for the first block, $p = 1$ and it can directly write as $(A_i^c - A_{i+1}^c)^T$. Take the trace of both sides of equation (43) and we have

$$\text{tr}(R^{-1} \widetilde{\mathcal{B}} \widetilde{\mathcal{A}}_i \widetilde{Q} \widetilde{H}_i \widetilde{\mathcal{A}}_i^c) = \text{vec}(R^{-1})^T \underbrace{(\widetilde{\mathcal{A}}_i^c \otimes \widetilde{\mathcal{B}} \widetilde{\mathcal{A}}_i)}_{\mathcal{E}_i} \text{vec}(\widetilde{Q} \widetilde{H}_i). \quad (44)$$

Notice that there are many zero elements and identical matrices in $\widetilde{Q} \widetilde{H}_i$ and R^{-1} . Therefore, the trace equation (44) can be simplified through the following three steps:

i) Let the set of indices of all non-zero elements in $\text{vec}(\widetilde{Q} \widetilde{H}_i)$ be \mathcal{C}_1 . Collect all the columns of \mathcal{E}_i with indices in \mathcal{C}_1 and form $\mathcal{P}_i^1(\mathcal{E}_i) = \mathcal{E}_i(:, \mathcal{C}_1)$. Then we have

$$\text{vec}(R^{-1})^T \mathcal{P}_i^1(\mathcal{E}_i) [\mathbf{1}_{N-i-1}^T \otimes \text{vec}(Q)^T, \text{vec}(H)^T, \text{vec}(H)^T]^T.$$

ii) Since $\text{vec}(Q)$ and $\text{vec}(H)$ appear multiple times, we define $\mathcal{P}_i^2(\mathcal{E}_i)$, where

$$\begin{aligned} \mathcal{P}_i^2(\mathcal{E}_i)(:, 1:n) &= \sum_{t=1}^{N-i-1} \mathcal{P}_i^1(\mathcal{E}_i)(:, 1+m(t-1):mt), \\ \mathcal{P}_i^2(\mathcal{E}_i)(:, n+1:2n) &= \sum_{t=N-i}^{N-i+1} \mathcal{P}_i^1(\mathcal{E}_i)(:, 1+m(t-1):mt). \end{aligned}$$

iii) Since $H, Q \in \mathbb{R}^n$ and $R \in \mathbb{R}^m$ are symmetric, we only need the upper triangle part $\text{vec}(\overline{H}), \text{vec}(\overline{Q}), \text{vec}(\overline{R^{-1}})$ respectively to uniquely determine them. We can further simplify (44) as

$$\begin{aligned} &\text{vec}(\overline{R^{-1}})^T \mathcal{P}_i(\mathcal{E}_i) \begin{bmatrix} \text{vec}(\overline{Q}) \\ \text{vec}(\overline{H}) \end{bmatrix} \\ &= ([\text{vec}(\overline{Q})^T, \text{vec}(\overline{H})^T] \otimes \text{vec}(\overline{R^{-1}})^T) \text{vec}(\mathcal{P}_i(\mathcal{E}_i)) \\ &= ([\text{vec}(\overline{Q}')^T, \text{vec}(\overline{H}')^T] \otimes \text{vec}(\overline{R'^{-1}})^T) \text{vec}(\mathcal{P}_i(\mathcal{E}_i)), \end{aligned} \quad (45)$$

where $\mathcal{P}_i(\mathcal{E}_i)$ is a $\frac{m(m+1)}{2} \times n(n+1)$ matrix.

If there exist at least $\frac{mn(n+1)(m+1)}{2}$ linearly independent vectors $\text{vec}(\mathcal{P}_i(\mathcal{E}_i))$ in the horizon $k = 0, \dots, N-1$, then we can combine them as a full row rank matrix and obtain

$$\begin{aligned} \text{vec}(\overline{Q}') &= \alpha \cdot \text{vec}(\overline{Q}), \text{vec}(\overline{H}') = \alpha \cdot \text{vec}(\overline{H}), \\ \text{vec}(\overline{R'^{-1}}) &= \frac{1}{\alpha} \cdot \text{vec}(\overline{R^{-1}}). \end{aligned}$$

Thus, we have $H' = \alpha H, Q' = \alpha Q, R' = \alpha R$. Note that if the matrix H, Q, R are all diagonal matrices, which is a common setting in practical scenarios, we only need $2nm$ linearly independent $\text{vec}(\mathcal{P}_i(\mathcal{E}_i))$.

APPENDIX E PROOF OF LEMMA 4

In this proof we will show how to obtain the equation (20) from the iterations of P_k, K_k . Transform the formula (13):

$$\begin{aligned} (13) &\Leftrightarrow (R + B^T P_{k+1} B) K_k = B^T P_{k+1} A, \\ &\Leftrightarrow R K_k = B^T P_{k+1} (A - B K_k) = B^T P_{k+1} A_k^c. \end{aligned}$$

Since $P_N = H$, for $k = N-1$ we have

$$R K_{N-1} = B^T H A_{N-1}^c \Leftrightarrow a_1 R b_1 = c_1 H d_1$$

where $a_1 = I_2, b_1 = K_{N-1}, c_1 = B^T$ and $d_1 = A_{N-1}^c$. For $k = N-2$ there is

$$R K_{N-2} = B^T P_{N-1} A_{N-2}^c$$

and substitute P_{N-1} with (14)

$$\begin{aligned} R K_{N-2} &= B^T (K_{N-1}^T R K_{N-1} + A_{N-1}^c{}^T H A_{N-1}^c + Q) A_{N-2}^c \\ &\Leftrightarrow \underbrace{[I_2 \quad -B^T K_{N-1}^T]}_{a_2} (I_2 \otimes R) \underbrace{\begin{bmatrix} K_{N-2} \\ K_{N-1} A_{N-2}^c \end{bmatrix}}_{b_2} = \\ &\underbrace{[B^T A_{N-1}^c{}^T \quad B^T]}_{c_2} \begin{bmatrix} H \\ Q \end{bmatrix} \underbrace{\begin{bmatrix} A_{N-1}^c A_{N-2}^c \\ A_{N-2}^c \end{bmatrix}}_{d_2}. \end{aligned}$$

For $k = N-3$ we have

$$\begin{aligned} R K_{N-3} &= B^T P_{N-2} A_{N-3}^c \\ &= B^T (K_{N-2}^T R K_{N-2} + A_{N-2}^c{}^T P_{N-1} A_{N-2}^c + Q) A_{N-3}^c \\ &= B^T (K_{N-2}^T R K_{N-2} + A_{N-2}^c{}^T (K_{N-1}^T R K_{N-1} \\ &\quad + A_{N-1}^c{}^T H A_{N-1}^c + Q) A_{N-2}^c + Q) A_{N-3}^c, \end{aligned}$$

which can also be transformed into the form

$$a_3 (I_3 \otimes R) b_3 = c_3 \begin{bmatrix} H \\ I_2 \otimes Q \end{bmatrix} d_3.$$

Therefore, according to the above derivation we conclude the equation (20) for $i = 1, \dots, N$, where the parameters a_i, b_i, c_i, d_i are calculated by (21).

APPENDIX F
PROOF OF THEOREM 5

a) We first studies the convergence of $\{P_k\}$ sequence. The following lemma provides a convergent property of algebraic Riccati equation.

Lemma 5. *There exist a constant $\gamma > 1$ and two non-negative constants $c_1 = c_1(\gamma, P_N, P_{N-1})$ and $c_2 = c_2(\gamma, P_N, P_{N-1})$ such that for any fixed finite control horizon N the following inequality holds for all $k = 0, 1, \dots, N-1$:*

$$\underline{\beta}_k P_{k+1} \leq P_k \leq \bar{\beta}_k P_{k+1}, \quad (46)$$

where

$$\underline{\beta}_k := \frac{\gamma^k(\gamma-1)}{\gamma^k(\gamma-1)+c_1}, \quad \bar{\beta}_k := \frac{\gamma^k(\gamma-1)+c_2}{\gamma^k(\gamma-1)}.$$

Proof. See the proof of Proposition 7 in [46]. \square

Lemma 5 reveals both monotonic and convergent properties of the $\{P_k\}$ sequence. Denote a positive definite matrix $\Phi = P_N^{-1/2} P_{N-1} P_N^{-1/2}$ and let

$$\begin{aligned} c_1 &= \max\{0, (\frac{1}{\lambda_{\min}(\Phi)} - 1)(\gamma-1)\}, \\ c_2 &= \max\{0, (\lambda_{\max}(\Phi) - 1)(\gamma-1)\}. \end{aligned} \quad (47)$$

The corresponding parameter $\gamma := 1/(1-\sigma)$ is calculated as formula (16) in [46]. However, one basic assumptions of Lemma 5 is $Q > 0$, while our problem may have $Q = 0$ (in Sec. III-B). If $Q = 0$, their calculation of parameter γ will fail and we provide the following selection method of γ instead.

Since the sequence $\{P_k\}$ is monotonic, we will discuss two kinds of conditions: increasing and decreasing. Firstly, we have

$$\begin{aligned} P_k - (A - BK_k)^T P_{k+1} (A - BK_k) &= K_k^T R K_k = A^T \\ P_{k+1}^T B (R + B^T P_{k+1} B)^{-T} R (R + B^T P_{k+1} B)^{-1} B^T P_{k+1} A. \end{aligned}$$

i) If the sequence $\{P_k\}$ is monotonically decreasing, there is $P_N \geq P_k \geq P^*$ for all k . Thus we have

$$\begin{aligned} P_k - (A - BK_k)^T P_{k+1} (A - BK_k) \\ \geq A^T P^* B (R + B^T P_N B)^{-T} R (R + B^T P_N B)^{-1} B^T P^* A \\ := Q_a > 0. \end{aligned}$$

ii) If the sequence $\{P_k\}$ is monotonically increasing, there is $P_N \leq P_k \leq P^*$ for all k . Thus we have

$$\begin{aligned} P_k - (A - BK_k)^T P_{k+1} (A - BK_k) \\ \geq A^T P_N B (R + B^T P^* B)^{-T} R (R + B^T P^* B)^{-1} B^T P_N A \\ := Q_b > 0. \end{aligned}$$

Therefore, let

$$\Gamma := \frac{1}{\kappa} \cdot Q_a \text{ (or } Q_b), \quad \sigma = \lambda_{\min}(\Gamma).$$

Select $\gamma := 1/(1-\sigma)$ and we have $\gamma > 1$.

b) We will then figure out the convergence property of $\{K_k\}$ with Lemma 5. Similarly, we discuss the following two monotonic situations separately:

i) If $P_N \leq P_{N-1}$ holds, we have $c_1 = 0, c_2 \geq 0$ and $P_k \leq P_{k-1} \leq \bar{\beta}_k P_{k+1}$ for all k , which yields that

$$\begin{aligned} P_k - P_{k+1} &\leq \bar{\beta}_k P_{k+1} - P_{k+1} \\ &\leq (\bar{\beta}_k - 1) P_{k+1} \leq (\bar{\beta}_k - 1) P_N. \end{aligned}$$

Then $\|P_k - P_{k+1}\| \leq (\bar{\beta}_k - 1) \|P_N\|$. There always exists $N_a \in \mathbb{N}_+$ and $\epsilon > 0$, for any $N > N_a$, we obtain $\|P_1 - P_0\| \leq \epsilon$.

$$\begin{aligned} \|K_0 - K_1\| &= \|(R + B^T P_1 B)^{-1} B^T P_1 A - (R + B^T P_2 B)^{-1} B^T P_2 A\| \\ &\leq \|(R + B^T P_2 B)^{-1} B^T (P_1 - P_2) A\| \\ &\leq \|(R + B^T P_N B)^{-1} B^T\| \cdot \|P_1 - P_2\| \cdot \|A\| =: \eta_a \end{aligned}$$

ii) If $P_N \geq P_{N-1}$ holds, we have $c_1 \geq 0, c_2 = 0$ and $\underline{\beta}_k P_{k+1} \leq P_k \leq P_{k+1}$ for all k , which yields that

$$\begin{aligned} P_{k+1} - P_k &\leq P_{k+1} - \underline{\beta}_k P_{k+1} \\ &\leq (1 - \underline{\beta}_k) P_{k+1} \leq (1 - \underline{\beta}_k) P_N. \end{aligned}$$

Then $\|P_{k+1} - P_k\| \leq (1 - \underline{\beta}_k) \|P_N\|$. There always exists $N_b \in \mathbb{N}_+$ and $\epsilon > 0$, for any $N > N_b$, we obtain $\|P_1 - P_0\| \leq \epsilon$.

$$\begin{aligned} \|K_1 - K_0\| &= \|(R + B^T P_2 B)^{-1} B^T P_2 A - (R + B^T P_1 B)^{-1} B^T P_1 A\| \\ &\leq \|(R + B^T P_1 B)^{-1} B^T (P_2 - P_1) A\| \\ &\leq \|(R + B^T P^* B)^{-1} B^T\| \cdot \|P_2 - P_1\| \cdot \|A\| =: \eta_b \end{aligned}$$

c) Based on previous discussion, we provide the proof of Theorem 5. When $N > \bar{N} = N_a$ (or N_b), there is

$$\begin{aligned} \|\mu_0^{(N+\delta N)} - \mu_0^{(N)}\| &= \|K_0^{(N+\delta N)} - K_0^{(N)}\| \cdot \|x_0\| \\ &= \|K_0^{(N+\delta N)} - K_{\delta N}^{(N+\delta N)}\| \cdot \|x_0\| \\ &\leq \delta N \|K_0^{(N+\delta N)} - K_1^{(N+\delta N)}\| \cdot \|x_0\| \\ &\leq \delta N \cdot \eta_a \text{ (or } \eta_b) \cdot \|x_0\| =: \eta. \end{aligned}$$

The proof is done.

REFERENCES

- [1] C. Qu, J. He, X. Duan, and S. Wu, "Control input inference of mobile agents under unknown objective," in *IFAC 2023 World Congress*, to be published, 2023.
- [2] J. Cao and S. K. Das, "Mobile agents and applications in networking and distributed computing," *Mobile Agents in Networking and Distributed Computing*, pp. 1-16, 2012.
- [3] S. G. Tzafestas, "Mobile robot control and navigation: A global overview," *Journal of Intelligent & Robotic Systems*, vol. 91, pp. 35-58, 2018.
- [4] L. Zhou and V. Kumar, "Robust multi-robot active target tracking against sensing and communication attacks," *IEEE Transactions on Robotics*, vol. 39, no. 3, pp. 1768-1780, 2023.
- [5] F. Pasqualetti, F. Dörfler, and F. Bullo, "Attack detection and identification in cyber-physical systems," *IEEE Transactions on Automatic Control*, vol. 58, no. 11, pp. 2715-2729, 2013.
- [6] C. Wu, W. Yao, W. Luo, W. Pan, G. Sun, H. Xie, and L. Wu, "A secure robot learning framework for cyber attack scheduling and countermeasure," *IEEE Transactions on Robotics*, 2023.

- [7] H. Ravichandar, A. S. Polydoros, S. Chernova, and A. Billard, "Recent advances in robot learning from demonstration," *Annual Review of Control, Robotics, and Autonomous Systems*, vol. 3, pp. 297–330, 2020.
- [8] W. Jin, T. D. Murphey, D. Kulić, N. Ezer, and S. Mou, "Learning from sparse demonstrations," *IEEE Transactions on Robotics*, vol. 39, no. 1, pp. 645–664, 2022.
- [9] M. Kuderer, S. Gulati, and W. Burgard, "Learning driving styles for autonomous vehicles from demonstration," in *2015 IEEE International Conference on Robotics and Automation (ICRA)*. IEEE, 2015, pp. 2641–2646.
- [10] D. Kent, M. Behrooz, and S. Chernova, "Construction of a 3d object recognition and manipulation database from grasp demonstrations," *Autonomous Robots*, vol. 40, pp. 175–192, 2016.
- [11] G. J. Maeda, G. Neumann, M. Ewerton, R. Lioutikov, O. Kroemer, and J. Peters, "Probabilistic movement primitives for coordination of multiple human–robot collaborative tasks," *Autonomous Robots*, vol. 41, pp. 593–612, 2017.
- [12] R. Rahmatizadeh, P. Abolghasemi, L. Bölöni, and S. Levine, "Vision-based multi-task manipulation for inexpensive robots using end-to-end learning from demonstration," in *2018 IEEE International Conference on Robotics and Automation (ICRA)*. IEEE, 2018, pp. 3758–3765.
- [13] F. Torabi, G. Warnell, and P. Stone, "Behavioral cloning from observation," *arXiv preprint arXiv:1805.01954*, 2018.
- [14] A. Bemporad, M. Morari, V. Dua, and E. N. Pistikopoulos, "The explicit linear quadratic regulator for constrained systems," *Automatica*, vol. 38, no. 1, pp. 3–20, 2002.
- [15] N. Ab Azar, A. Shahmansoorian, and M. Davoudi, "From inverse optimal control to inverse reinforcement learning: A historical review," *Annual Reviews in Control*, vol. 50, pp. 119–138, 2020.
- [16] W. Jin, D. Kulić, J. F.-S. Lin, S. Mou, and S. Hirche, "Inverse optimal control for multiphase cost functions," *IEEE Transactions on Robotics*, vol. 35, no. 6, pp. 1387–1398, 2019.
- [17] B. D. Anderson and J. B. Moore, *Optimal control: Linear quadratic methods*. Courier Corporation, 2007.
- [18] M. C. Priess, R. Conway, J. Choi, J. M. Popovich, and C. Radcliffe, "Solutions to the inverse lqr problem with application to biological systems analysis," *IEEE Transactions on Control Systems Technology*, vol. 23, no. 2, pp. 770–777, 2014.
- [19] E. Pauwels, D. Henrion, and J.-B. Lasserre, "Linear conic optimization for inverse optimal control," *SIAM Journal on Control and Optimization*, vol. 54, no. 3, pp. 1798–1825, 2016.
- [20] Y. Li, Y. Yao, and X. Hu, "Continuous-time inverse quadratic optimal control problem," *Automatica*, vol. 117, p. 108977, 2020.
- [21] C. Yu, Y. Li, H. Fang, and J. Chen, "System identification approach for inverse optimal control of finite-horizon linear quadratic regulators," *Automatica*, vol. 129, p. 109636, 2021.
- [22] H. Zhang, J. Umenberger, and X. Hu, "Inverse optimal control for discrete-time finite-horizon linear quadratic regulators," *Automatica*, vol. 110, p. 108593, 2019.
- [23] J. A. Primbs and V. Nevistić, "Feasibility and stability of constrained finite receding horizon control," *Automatica*, vol. 36, no. 7, pp. 965–971, 2000.
- [24] E. Bøhn, S. Gros, S. Moe, and T. A. Johansen, "Reinforcement learning of the prediction horizon in model predictive control," *IFAC-PapersOnLine*, vol. 54, no. 6, pp. 314–320, 2021.
- [25] Z. Sun, L. Dai, K. Liu, D. V. Dimarogonas, and Y. Xia, "Robust self-triggered mpc with adaptive prediction horizon for perturbed nonlinear systems," *IEEE Transactions on Automatic Control*, vol. 64, no. 11, pp. 4780–4787, 2019.
- [26] J. Chen, T. Liu, and S. Shen, "Tracking a moving target in cluttered environments using a quadrotor," in *2016 IEEE/RSJ International Conference on Intelligent Robots and Systems (IROS)*. IEEE, 2016, pp. 446–453.
- [27] F. Gao, W. Wu, Y. Lin, and S. Shen, "Online safe trajectory generation for quadrotors using fast marching method and bernstein basis polynomial," in *2018 IEEE International Conference on Robotics and Automation (ICRA)*. IEEE, 2018, pp. 344–351.
- [28] F. Alché and A. de La Fortelle, "An lstm network for highway trajectory prediction," in *2017 IEEE 20th International Conference on Intelligent Transportation Systems (ITSC)*. IEEE, 2017, pp. 353–359.
- [29] A. Mohamed, K. Qian, M. Elhoseiny, and C. Claudel, "Social-stgenn: A social spatio-temporal graph convolutional neural network for human trajectory prediction," in *Proceedings of the IEEE/CVF Conference on Computer Vision and Pattern Recognition (CVPR)*, 2020, pp. 14424–14432.
- [30] J. Schulz, C. Hubmann, J. Löchner, and D. Burschka, "Multiple model unscented Kalman filtering in dynamic Bayesian networks for intention estimation and trajectory prediction," in *2018 IEEE 21st International Conference on Intelligent Transportation Systems (ITSC)*. IEEE, 2018, pp. 1467–1474.
- [31] J. Li, J. He, Y. Li, and X. Guan, "Unpredictable trajectory design for mobile agents," in *2020 American Control Conference (ACC)*. IEEE, 2020, pp. 1471–1476.
- [32] L. Ljung, "System identification," in *Signal Analysis and Prediction*. Springer, 1998, pp. 163–173.
- [33] G. Welch, G. Bishop *et al.*, "An introduction to the Kalman filter," 1995.
- [34] S. Gillijns and B. De Moor, "Unbiased minimum-variance input and state estimation for linear discrete-time systems," *Automatica*, vol. 43, no. 1, pp. 111–116, 2007.
- [35] T. L. Molloy, D. Tsai, J. J. Ford, and T. Perez, "Discrete-time inverse optimal control with partial-state information: A soft-optimality approach with constrained state estimation," in *2016 IEEE 55th Conference on Decision and Control (CDC)*. IEEE, 2016, pp. 1926–1932.
- [36] Y. Li, J. He, C. Chen, and X. Guan, "Topology inference for network systems: Causality perspective and non-asymptotic performance," *IEEE Transactions on Automatic Control*, to be published, 2023.
- [37] D. Bertsekas, *Dynamic programming and optimal control: Volume I*. Athena Scientific, 2012, vol. 1.
- [38] P. H. Richter, "Estimating errors in least-squares fitting," *The Telecommunications and Data Acquisition Report*, 1995.
- [39] B. Stellato, G. Banjac, P. Goulart, A. Bemporad, and S. Boyd, "Osqp: An operator splitting solver for quadratic programs," *Mathematical Programming Computation*, vol. 12, no. 4, pp. 637–672, 2020.
- [40] H. Kwakernaak and R. Sivan, "The maximally achievable accuracy of linear optimal regulators and linear optimal filters," *IEEE Transactions on Automatic Control*, vol. 17, no. 1, pp. 79–86, 1972.
- [41] R. Bellman, "Dynamic programming," *Science*, vol. 153, 1966.
- [42] R. R. Bitmead and M. Gevers, "Riccati difference and differential equations: Convergence, monotonicity and stability," *The Riccati Equation*, pp. 263–291, 1991.
- [43] J. Lofberg, "Yalmip: A toolbox for modeling and optimization in matlab," in *2004 IEEE International Conference on Robotics and Automation (ICRA)*. IEEE, 2004, pp. 284–289.
- [44] J. F. Sturm, "Using sedumi 1.02, a matlab toolbox for optimization over symmetric cones," *Optimization Methods and Software*, vol. 11, no. 1–4, pp. 625–653, 1999.
- [45] X. Ding, H. Wang, H. Li, H. Jiang, and J. He, "Robopheus: A virtual-physical interactive mobile robotic testbed," 2021.
- [46] X. Cai, Y. Ding, and S. Li, "Convergent properties of riccati equation with application to stability analysis of state estimation," *Mathematical Problems in Engineering*, vol. 2017, 2017.

Chendi Qu received the B.E. degree in the Department of Automation from Tsinghua University, Beijing, China, in 2021. She is currently working toward the Ph.D. degree with the Department of Automation, Shanghai Jiao Tong University, Shanghai, China. She is a member of Intelligent Wireless Networks and Cooperative Control group. Her research interests include robotics, security of cyber-physical system, and distributed optimization and learning in multi-agent networks.

Jianping He (SM'19) is an Associate Professor in the Department of Automation at Shanghai Jiao Tong University. He received the Ph.D. degree in control science and engineering from Zhejiang University, Hangzhou, China, in 2013, and had been a research fellow in the Department of Electrical and Computer Engineering at University of Victoria, Canada, from Dec. 2013 to Mar. 2017. His research interests mainly include the distributed learning, control and optimization, security and privacy in network systems.

Dr. He serves as an Associate Editor for IEEE Trans. Control of Network Systems, IEEE Open Journal of Vehicular Technology, and KSII Trans. Internet and Information Systems. He was also a Guest Editor of IEEE TAC, IEEE TII, International Journal of Robust and Nonlinear Control, etc. He was the winner of Outstanding Thesis Award, Chinese Association of Automation, 2015. He received the best paper award from IEEE WCSP'17, the best conference paper award from IEEE PESGM'17, and was a finalist for the best student paper award from IEEE ICCA'17, and the finalist best conference paper award from IEEE VTC'20-FALL.

Xiaoming Duan is an assistant professor in the Department of Automation at Shanghai Jiao Tong University. He obtained his B.E. degree in Automation from the Beijing Institute of Technology in 2013, his Master's Degree in Control Science and Engineering from Zhejiang University in 2016, and his Ph.D. degree in Mechanical Engineering from the University of California at Santa Barbara in 2020. He was a postdoctoral fellow in the Oden Institute for Computational Engineering and Sciences at the University of Texas at Austin in 2021. His research interests include robotics, multi-agent systems, and autonomous systems.